Fluorescence Lifetime Correlation Spectroscopic Study of Fluorophore-Labeled Silver Nanoparticles

Krishanu Ray,* Jian Zhang, and Joseph R. Lakowicz

Center for Fluorescence Spectroscopy, Department of Biochemistry and Molecular Biology, University of Maryland School of Medicine, 725 West Lombard Street, Baltimore, Maryland 21201

In this paper, we introduce the use of fluorescence lifetime correlation spectroscopy to study the metal–fluorophore interactions in solution at the single-fluorophore level. A single-stranded oligonucleotide was chemically bound to a 50-nm-diameter single silver particle, and a Cy5-labeled complementary single-stranded oligonucleotide was hybridized with the silver particle-bound oligonucleotide. The distance between the fluorophore and silver particle was maintained by a rigid hybridized DNA duplex of 8 nm in length. The single Cy5-DNA-Ag particles showed more than 10-fold increase in fluorescence intensity and a 5-fold decrease in emission lifetimes as compared with Cy5-DNA free molecules in the absence of metal. The decrease of lifetime for the Cy5-DNA-Ag particle allowed us to resolve the correlation functions of the two species based on the intensity decays. The increased brightness of the Cy5-DNA-Ag particle as compared to free Cy5-DNA resulted in an increased contribution of Cy5-DNA-Ag to the correlation function of the mixture. These results show that the effects of metal particles on fluorophores can be used to detect the small fractional populations of the metal-bound species in the presence of a larger number of less bright species. Our results also suggest that these bright fluorophores conjugated to silver particles could be used as the fluorescent probes for clinical detection in the biological samples with the high background.

Fluorescence detection is the basis of many measurements in biological research and clinical diagnosis including studies of biological macromolecules, cell imaging, DNA sequencing, and drug discovery. In recent years, there has been a growing interest in the interactions of fluorophores with metallic surfaces or nanoscale metallic particles.[1–14] The spectral properties of fluorophores can be dramatically altered by near-field interactions with the electron clouds present in the metals. Fluorophores in the excited state can create plasmons that radiate into the far field, and the fluorophores in the ground state can interact with or can be excited by the surface plasmons created by incident light.[1–9] These reciprocal interactions suggest that the novel optical absorption and scattering properties of metallic nanostructures can be used to control the decay rates, location, and direction of fluorophore emission. Metal particles can be used to increase the fluorescence intensities via a combination of enhanced fields around the metal nanoparticles and a rapid and efficient emission from the metal–fluorophore system.[3] This effect is called metal-enhanced fluorescence (MEF), which typically results in increased intensities and decreased lifetimes.

Fluorescence lifetime correlation spectroscopy (FLCS)[15–19] is a newly developed method that combines two well-established techniques, fluorescence correlation spectroscopy (FCS)[20–22] and time-correlated single-photon counting (TCSPC). By FLCS, different fluorescence contributions are statistically separated on a single-photon level. In this method, a separate autocorrelation function is created for each emission lifetime component resulting from different fluorescent species rather than fitting complex autocorrelation function with a multiparameter model. The resolution of the measured autocorrelation function with two or more separate functions is possible because of the additional intensity decay information. This resolution assumes that individual intensity decay is in fact associated with its own correlation function, that is, separate diffusing species with distinct intensity decays.

(10) Vasilev, K.; Knoll, W.; Kreiter, M. *J. Chem. Phys.* **2004**, *120*, 3439–3445.
(11) Yonzon, C. R.; Jeoung, E.; Zou, S.; Schatz, G. C.; Mrksich, M.; Van, Duyne, R. P. *J. Am. Chem. Soc.* **2004**, *126*, 12669–126676.
(12) Song, J.-H.; Atay, T.; Shi, S.; Urabe, H.; Nurmikko, A. V. *Nano Lett.* **2005**, *5*, 1557–1561.
(13) Antunes, P. A.; Constantino, C. J. L.; Aroca, R. F.; Duff, J. *Langmuir* **2001**, *17*, 2958–2964.
(14) Sokolov, K.; Chumanov, G.; Cotton, T. M. *Anal. Chem.* **1998**, *70*, 3898–3905.
(15) Gregor, I.; Enderlein. *J. Photochem. Photobiol. Sci.* **2007**, *6*, 13.
(16) Benda, A.; Fagulova, V.; Deyneka, A.; Enderlein, J.; Hof, M. *Langmuir* **2006**, *22*, 9580–9585.
(17) Enderlein, J.; Gregor, I. *Rev. Sci. Instrum.* **2005**, *76*, 033102.
(18) Kapusta, P.; Wahl, M.; Benda, A.; Hof, M.; Enderlein, J. *J. Fluoresc.* **2007**, *17*, 43–48.
(19) Bohmer, M.; Wahl, M.; Hans-Jurgen, R.; Erdmann, R.; Enderlein, J. *Chem. Phys. Lett.* **2002**, *353*, 439–445.
(20) Rigler, R.; Elson, E. *Fluorescence Correlation Spectroscopy: Theory and Applications*; Springer: Berlin, 2001.
(21) Maiti, S.; Haupts, U.; Webb, W. W. *Proc. Natl. Acad. Sci.U. S. A.* **1997**, *94*, 11753.
(22) Laurence, T. A.; Kwon, Y.; Yin, E.; Hollars, C. W.; Camarero, J. A.; Barsky, D. *Biophys. J.* **2007**, *92*, 2184–2198.

(1) Fort, E.; Gresillon, S. *J. Phys. D. Appl. Phys.* **2008**, *41*, 013001.
(2) Lakowicz, J. R. *Anal. Biochem.* **2005**, *337*, 171–194.
(3) Lakowicz, J. R. *Plasmonics* **2006**, *1*, 5–33.
(4) Ray, K.; Badugu, R.; Lakowicz, J. R. *J. Am. Chem. Soc.* **2006**, *128*, 8998–8999.
(5) Yokota, H.; Saito, K.; Yanagida, T. *Phys. Rev. Lett.* **1998**, *80*, 4606–4609.
(6) Mertens, H.; Koenderink, A. F.; Polman, A. *Phys. Rev. B* **2007**, *76*, 115123.
(7) Anger, P.; Bharadwaj, P.; Novotny, L. *Phys. Rev. Lett.* **2006**, *96*, 113002.
(8) Kuhn, S.; Hakason, U.; Rogobete, L.; Sandoghdar, V. *Phys. Rev. Lett.* **2006**, *97*, 017402.
(9) Tam, F.; Goodrich, G. P.; Johnson, B.; Halas, N. J. *Nano Lett.* **2007**, *7*, 496–501.

Scheme 1. Succinimidylated Silver Particle Covalently Bound with Aminated Single-Stranded Oligonucleotide and Fluorescently Labeled by Complementary Single-Stranded Cy5-Labeled Oligonucleotide[a]

Aminated oligo: H₂N-3'-TCCACACACCACTGGCCATCTTG-5'

Labeled oligo: 3'-AGGTGTGTGGTGACCGGTAGAAC-Cy5-5'

[a] Oligonucleotide sequences used in the experiments are given.

In this paper, we describe the use of FLCS with picosecond time-resolved detection to separate the FCS contributions from fluorophores and metal-conjugated fluorophores in solution. The size effect of silver particle on the photophysics of bound Cy5-labeled DNA ranging in diameter from 5 to 100 nm was reported at a single-molecule level.[23,24] The brightness of the Cy5 molecule strongly depends on the silver particle size. The highest enhancement in intensity and photostability appeared to occur with the 50−70-nm-diameter particle.[23,24] For this reason, we bound Cy5-DNA bound to a 50-nm silver particle (Cy5-DNA-Ag particle) and used FLCS to investigate the MEF of these metal-conjugated fluorophores. To the best of our knowledge, this is the first FCS study of a fluorophore conjugated to a metal nanoparticle in solution at the single-molecule level. This is also the first study where FLCS is being applied to a system where the brightness and the fluorescent lifetime of the emitting species are significantly different. In order to investigate the dynamics of single molecules by fluorescence correlation spectroscopy, it requires that the rate of photon detection per molecule be high, and the background is low. In this regard, these metal-nanoparticle conjugated fluorophores offer to be excellent probes to meet those requirements.

EXPERIMENTAL SECTION

Materials. All reagents and spectroscopic grade solvents were used as received from Fisher or Aldrich. RC dialysis membrane (MWCO 50 000) was obtained from Spectrum Laboratories, Inc. Nanopure water (>18.0 MΩ·cm) purified using the Millipore Milli-Q gradient system, was used in all experiments. (2-Mercaptopropionylamino)acetic acid-2,5-dioxopyrrolidin-1-yl ester was synthesized as previously reported.[25] Oligonucleotides (Scheme 1) were synthesized by the Biopolymer Laboratory at the University of Maryland at Baltimore, in which aminated oligonucleotide was also synthesized with one amino group substituted on the pyrimidine ring of a thymine base and the complementary oligonucleotide was labeled by Cy5.

Preparation of Succinimidylated Tiopronin-Coated Metal Nanoparticles. Tiopronin-coated silver nanoparticles with 50-nm diameter were prepared by chemical reduction of silver nitrate

using ascorbic acid.[26] These silver particles were succinimidylated by ligand exchange. (2-mercaptopropionylamino)acetic acid-2,5-dioxo-pyrrolidin-1-yl ester and tiopronin-coated silver particles were codissolved in water at a molar ratio of 1/2.[27]

The synthesized water-soluble silver particles are coated by the thiolate ligands. The results from other laboratories and us reveal that these metal particles are chemically stable in the surface modifications and the measurements to their optical and electrochemical properties.[26,27] Because of the stronger sulfur and metal bonds, the thiolate ligand-protected metal particles are expected to be more stable as compared with the citrate-coated metal particles.

Binding and Hybridizing Oligonucleotides on Silver Nanoparticles. Aminated oligonucleotides were covalently bound onto the silver particles by condensation between the amino moieties on the oligonucleotides and the terminal succinimidyl ester moieties on the silver particles.[26] The oligonucleotides and succinimidylated metal particles were codissolved in water at a molar ratio of 1/1 with continuous stirring for 24 h. The metal particles were centrifuged at 6000 rpm to remove the unbound oligonucleotides in suspension. The residue was washed with water and dispersed in 50 mM PBS buffer solution at pH 7.2.

The fluorophore-labeled complementary oligonucleotides were bound to the metal particles by hybridization with the bound oligonucleotides,[25,26,29,30] which were performed at a molar ratio of particle/labeled oligonucleotide = 1/1. The supernatant was removed by centrifugation at 6000 rpm. The residual particles were washed with the buffer and then dialyzed against the buffer solution (MWCO 50 000) to remove any unbound impurities for the spectral measurements.

Transmission Electron Microscopy (TEM) Measurements. Transmission electron micrographs were taken with a side-entry Philips electron microscope at 120 keV. Samples were cast from water solutions onto standard carbon-coated (200−300 Å) Formvar films on copper grids (200 mesh) by placing a droplet of a 1 mg/

(23) Zhang, J.; Fu, Y.; Chowdhury, M. H.; Lakowicz, J. R. *J. Phys. Chem. C* **2008**, *112*, 18−26.

(24) Zhang, J.; Fu, Y.; Chowdhury, M. H.; Lakowicz, J. R. *Nano Lett.* **2007**, *7*, 2101−2107.

(25) Zhang, J.; Roll, D.; Geddes, C. D.; Lakowicz, J. R. *J. Phys. Chem. B* **2004**, *108*, 12210−12214.

(26) Zhang, J.; Fu, Y.; Chowdhury, M. H.; Lakowicz, J. R. *J. Phys. Chem. C* **2007**, *111*, 11784−11792.

(27) Templeton, A. C.; Wuelfing, W. P.; Murray, R. W. *Acc. Chem. Res.* **2000**, *33*, 27−36.

(28) Ingram, R. S.; Hostetler, M. J.; Murray, R. W. *J. Am. Chem. Soc.* **1997**, *119*, 9175−9178.

(29) Ambrose, W. P.; Goodwin, P. M.; Jett, J. H.; Van Orden, A.; Werner, J. H.; Keller, R. A. *Chem. Rev.* **1999**, *99*, 2929−2956.

(30) Willets, K. A.; Nishimura, S. Y.; Schuck, P. J.; Twieg, R. J.; Moerner, W. E. *Acc. Chem. Res.* **2005**, *38*, 549−556.
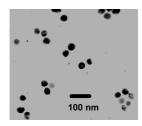
Figure 1. Transmission electron microscopy image of the 50-nm silver particles.

mL aqueous sample solution on grids. The size distribution of metal core was analyzed with Scion Image Beta Release 2 counting at least 200 particles.

A representative TEM image (Figure 1) showed an average diameter of the metal cores to be 50 nm. The size distributions of metal particles were analyzed with Scion Image Beta Release 2 counting at least 200 TEM images showing that at least 80% of the metal particles were distributed in ranges of 50 ± 20 nm. Accordingly, an average chemical composition was about $(Ag)4 \times 10^6 (Tio)3 \times 10^4$.

Absorption and Emission Spectroscopy. Absorption spectra were recorded with a Hewlett-Packard 8453 spectrophotometer. Ensemble fluorescence spectra were recorded with a Varian Cary Eclipse Fluorescence Spectrophotometer.

Fluorescence Lifetime Correlation Spectroscopy Measurements.[15–19] FLCS measurements were performed using a scanning confocal time-resolved microscope (Picoquant MicroTime 200). The excitation laser ($\lambda_{ex} \sim 635$ nm) was reflected by a dichroic mirror to a high numerical aperture (NA) oil objective (100×, NA 1.3) and focused onto the solution sample. The fluorescence was collected by avalanche photodiodes through a dichroic beam splitter and a band-pass (650−720 nm, Chroma) filter, thus eliminating the scattered excitation light and collecting the fluorescence from the Cy5 probes in the region of interest. We have used a PicoQuant TimeHarp 200 PC board operated in time-tagged time-resolved mode. For fluorophore conjugated silver nanoparticles, we have obtained two different lifetime components. Calculations of time-correlated single-photon counting filtered autocorrelation of Cy5-DNA-Ag nanoparticles are performed with the PicoQuant Symphotime software (version 4.3).

The fluorescence intensity decays were analyzed in terms of the multiexponential model:[31]

$$I(t) = \sum_{i=1}^{n} \alpha_i \exp(-t/\tau_i) \tag{1}$$

where, τ_i are the lifetimes with amplitudes α_i and $\sum_i \alpha_i = 1.0$. The contribution of each component to the steady-state intensity is given by

$$f_i = \frac{\alpha_i \tau_i}{\sum_j \alpha_j \tau_j} \tag{2}$$

The average lifetime is represented by

(31) Lakowicz, J. R. *Principles of Fluorescence Spectroscopy,* 3rd ed.; Kluwer Academic/Plenum Publishers: New York, 2006.

$$\bar{\tau} = \sum_i f_i \tau_i \tag{3}$$

and the amplitude-weighted lifetime is given by

$$<\tau> = \sum_i \alpha_i \tau_i \tag{4}$$

The values of α_i and τ_i were determined using the PicoQuant Symphotime software with nonlinear least-squares fitting. The goodness-of-fit was determined by the χ^2 value.

Theory of Fluorescence Lifetime Correlation Spectroscopy. FLCS is a combination of fluorescence lifetime and FCS measurement.[15–19] In this measurement, the fluorescence excitation is accomplished with a pulsed laser, and the fluorescence photons are detected on two different times scales, so-called time-tagged time-correlated photon counting: on a pico- to nanosecond time scale, where the distance between the exciting laser pulses and the photon detection events is time stamped (TCSPC), and on a much larger time scale from 100 ns to seconds. The absolute arrival time of detected photons is recorded, which is subsequently used for calculating the autocorrelation function (ACF). For metal−fluorophore complex, we assume that there are two different lifetime components, in which the measured intensity signal I_j could be written as[15–19]

$$I_j(t) = w^1(t)p_j^1 + w^2(t)p_j^2 \tag{5}$$

where the index j refers to the jth discrete TCSPC time channel used for timing the photon detection events with respect to the exciting laser pulses, $p_j^{1,2}$ are the normalized fluorescence decay distributions over these channels for the two different fluorescence decay signatures of the sample (e.g., two monoexponential decays with different decay constant), and the $w_j^{1,2}(t)$ are the total intensities of both fluorescence contributions measured at a given time t of the macroscopic time scale. Two completely different times scales are involved in eq 5: the macroscopic time scale of t, on which the ACF is calculated, and the (discrete) TCSPC time scale labeled by the numbers j of the corresponding TCSPC time channel. Fluorescence decay-specific autocorrelation and cross-correlation functions can now be described as

$$g_{12}(t) = \langle w^1(t_0) w^2(t_0 + t) \rangle_{t_0} \tag{6}$$

where the broken brackets denote averaging over time t_0. $w^1(t)$ could be recovered from the measured $I_j(t)$ using the following expression:

$$w^1(t) = \sum_{j=1}^{N} F_j^1 I_j(t) \tag{7}$$

F is the filter function which is a $2 \times N$ matrix with elements F_j^1, $1 \leq j \leq N$. The autocorrelation and cross-correlation functions are given by

$$g_{12}(t) = \sum_{j=1}^{N} \sum_{k=1}^{N} F_j^1 F_k^2 \langle I_j(t_0 + t) I_k(t_0) \rangle_{t_0} \tag{8}$$
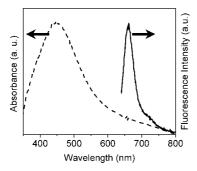
Figure 2. Absorbance spectrum of tiopronin-coated silver particles and ensemble emission spectra of Cy5-labeled oligonucleotide bound on the silver particles.

Calculations of TCSPC filtered autocorrelation of Cy5-DNA-Ag particles are performed using the above expression that contained within the PicoQuant Symphotime software (version 4.3).

RESULTS AND DISCUSSION

The tiopronin-coated silver particles were observed to display good solubility and chemical stability in water. The silver particles were succinimidylated by (2-mercaptopropionylamino)acetic acid-2,5-dioxo-pyrrolidin-1-yl ester via ligand exchange reaction at 1:1 molar ratio.[27,28] The succinimidyl ester and silver particle were codissolved in water at a molar ratio of 1/2 to display only a single succinimidyl ester molecule on each metal particle.[26] This treatment reduces the probability that the silver particles may be covalently bound by more than one oligonucleotide in the following surface reaction. The aminated single-stranded oligonucleotide was covalently bound to the succinimidylated metal particle via condensation. With only one succinimidyl ligand on each metal particle, we expected to covalently bind a single oligonucleotide molecule to a single silver particle in this surface reaction.

A single Cy5-labeled complementary oligonucleotide was hybridized with the bound oligonucleotide on the metal particle in 50 mM PBS buffer solution at pH 7.2.[25,26] The molar ratio of fluorophore/per metal particle was estimated quantitatively when dissolving the metal core with NaCN aqueous solution.[26] The released fluorophore-labeled oligonucleotide was observed to display an emission spectrum identical to that of the free oligonucleotide in the absence of metal, and the concentration of the released fluorophore was estimated from the emission intensity. The value was 0.3, indicating that about half amount of metal particles were bound by a single oligonucleotide. The above surface reactions on the silver particles did not significantly alter their absorbance spectra because only few reactive ligands were involved.

Figure 2 shows a plasmon absorbance at 454 nm for tiopronin-coated silver particles in water. Free Cy5-labeled oligonucleotide displayed an emission maximum at 661 nm upon excitation at 620 nm. The emission maximum of Cy5-DNA bound to a silver nanoparticle was slightly shifted to 662 nm (Figure 2). The hybridized DNA duplex chains separate the fluorophores from the metal cores. The DNA used in the current experiment contains 23 base pairs, so the separation between the fluorophore and metal core is ∼8 nm. This distance is approximately considered to be
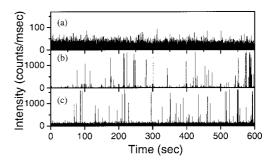

Figure 3. Intensity−time traces of (a) Cy5-DNA free (1 nM), (b) single Cy5-DNA-Ag particle (100 pM), and (c) mixture of Cy5-DNA-free (1 nM) and Cy5-DNA-Ag particle (100 pM) in water. Intensity scale bar is different between panels a, b, and c.
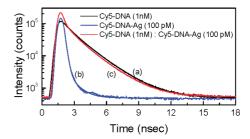

Figure 4. Intensity−time decays of (a) Cy5-DNA free (1 nM), (b) single Cy5-DNA-Ag particle (100 pM), and (c) mixture of Cy5-DNA-free (1 nM) and Cy5-DNA-Ag particle (100 pM) in water.

an optimized value for the most efficient metal-enhanced fluorescence.[2,32]

Figure 3 presents the emission intensity fluctuations of Cy5-DNA free (1 nM), Cy5-DNA-Ag particle, (100 pM), and a simple mixture of free Cy5-DNA and Cy5-DNA-Ag particle at a molar ratio of 1 nM:100 pM in water. We have observed a significant enhancement (more than 10-fold) of fluorescent signal (pulse height) from the Cy5-DNA-Ag particle sample compared to Cy5-DNA free sample. This effect can be seen from the increased intensities of the photon bursts from Cy5-DNA-Ag (Figure 3b) as compared to free Cy5-DNA (Figure 3a). This difference in intensity due to a single fluorophore allows the signal from Ag particle-conjugated Cy5 to be visually distinguished from the free Cy5-DNA sample (Figure 3c). The increased brightness of Cy5-DNA-Ag particle could be due to increased rates of excitation, emission, or more probably both. If the effects were due only to increased rates of excitation, then the lifetimes are expected to stay the same and the photostability is expected to decrease. However, we observed that the photostability increased[23,24] and the lifetime decreased, consistent with our expectation that both excitation and emission were involved in the enhancement process.[23,24]

The intensity decays obtained during the FCS measurements are presented in Figure 4. The Cy5-DNA-Ag particle showed a much faster decay with ∼5-fold decrease in average fluorescence lifetime (from ∼1.8 ns for free Cy5-DNA to 0.35 ns for Cy5-DNA-Ag particle). These unusual fluorescence properties, i.e., increase in fluorescence intensity and decrease in lifetime of Cy5-DNA-Ag particles, are thought to be due to the presence of enhanced local fields around the 50-nm silver particle and the increased emission rate of the metal−fluorophore conjugates. Besides the lifetime,

(32) Ray, K.; Badugu, R.; Lakowicz, J. R. *J. Phys. Chem. C* **2007**, *111*, 7091–7097.
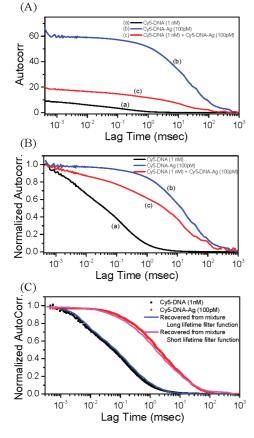
Figure 5. (A) Autocorrelation of (a) Cy5-DNA free, (b) bound to 50-nm silver particle, and (c) the mixture of Cy5-DNA free and Cy5-DNA-Ag in solution. (B) Normalized autocorrelation of Cy5-DNA free, bound to 50-nm silver particle, and the mixture of Cy5-DNA and Cy5-DNA-Ag. (C) Autocorrelation functions resolved based on lifetime.

the increase of emission intensity by the interaction of fluorophore with the metal particle can lead to an increase of the apparent quantum yield of the fluorophore. These effects provide an opportunity to resolve the individual species based on intensities and lifetimes.

Figure 5A shows the measured correlation functions for Cy5-DNA free (1 nM) and Cy5-DNA-Ag particle (100 pM) in solution. As expected, the correlation function for the bound Cy5 is strongly shifted to longer times because of the slower diffusion of the Cy5-DNA-Ag particle as compared to the free Cy5-DNA. The $G(0)$ intercept of the Ag particle sample is ~10-fold higher than free Cy5-DNA (not shown), which is consistent with the 10-fold lower concentration of the Cy5-DNA-Ag particle sample.

The autocorrelation curve for a mixture of 1 nM Cy5-DNA and 100 pM Cy5-DNA-Ag particle is also shown in Figure 5A and B. It is important to notice that this curve is shifted more than halfway toward the Ag particle-only curve, even though the Cy5-DNA-Ag particle concentration is 10-fold less than Cy5-DNA. This dominant contribution of the Ag particle-bound form, even with a 10-fold lower concentration of Cy5-DNA-Ag particle, is due to the higher brightness of Ag particle-bound Cy5-DNA as compared with free Cy5-DNA. The data can be used to recover the relative brightness of the two species, which can then be compared with similar data measured from individual species. For multiple diffusion species of diffusion coefficients D_1 and D_2, and the same brightness, the autocorrelation function is given by

$$G(\tau) = \frac{1}{N^2}[N_1 D_1(\tau) + N_2 D_2(\tau)] \tag{9}$$

where N_1 and N_2 are the number of free Cy5-DNA and Cy5-DNA-Ag particles and $N = N_1 + N_2$ is the total number of emitting species. The diffusion coefficient for the ith species traversing a 3D Gaussian volume with radius ω_0 and half-axial height z_0 is given by

$$D_i(\tau) = \left(1 + \frac{4D_i\tau}{\omega_0^2}\right)^{-1}\left(1 + \frac{4D_i\tau}{z_0^2}\right)^{-1/2} \tag{10}$$

If the diffusing species have different brightness, eq 9 can be rewritten as

$$G(\tau) = \frac{N_1 B_1^2 D_1(\tau) + N_2 B_2^2 D_2(\tau)}{(N_1 B_1 + N_2 B_2)^2} \tag{11}$$

where B_1 and B_2 are brightness of free Cy5-DNA and Cy5-DNA-Ag particles. The term brightness refers to the number of detected photons per time interval under the chosen experimental conditions. It is apparent from eq 11 that each species contributes to the autocorrelation function proportional to square of the brightness. As the brightness of Cy5-DNA-Ag particles are more than 10-fold higher than the free Cy5-DNA molecules, the autocorrelation function is strongly weighted by the brightest species (Cy5-DNA-Ag particle in the present case) in the sample volume as evident in Figure 5A and B. An advantage of FCS over single-molecule detection is that the fluorescence species are continually replaced by diffusion, and hence, the measurements can be continued as long as needed. In contrast, a surface-bound single molecule can only be studied only, when it is photobleached.

The intensity decays can be used with the data from a mixture to recover the separate correlation curves of each species in the mixture.[15–19] This resolution is possible because the entire time sequence of the photon counts is measured, so that the data contain not only the intensity fluctuations but also the time delays between the laser pulses and the arrival time of the photons. We have recovered two decay times from the mixture of free Cy5-DNA and of the Ag particle-bound form. The lifetimes resolved using the FCS data were similar to that of free Cy5-DNA and Cy5-DNA-Ag particle shown in Figure 4. Based on the intensity decay in Figure 4, we assign these values to the free and bound forms, respectively. With this assignment, we found that the recovered lifetime-resolved correlation curves are in good agreement with those measured for the individual species (Figure 5C).

In conclusion, we show that FLCS is a powerful tool to investigate the metal−fluorophore interactions at the single-molecule level and to separate multiple species with different lifetimes from a mixture solution. We have combined FLCS and MEF in the present study. We have demonstrated, for the first time, the metal-enhanced fluorescence from a fluorophore (Cy5) bound to a 50-nm-diameter silver colloid in solution by FLCS. In this measurement, the fluorescence brightness and lifetime of the emitting species are observed to alter significantly in solution at the single-molecule level, and the brightness of metal-conjugated fluorophore is enhanced to more than 10-fold and the lifetime is shortened to 5-fold simultaneously. The signal change can be

observed even at the 100 pM level, demonstrating that FLCS is a powerful method to investigate the biological targets separating two different species from a mixture solution emitting at the same wavelength at the single-molecule level. Our results also suggest that these highly bright silver particle conjugated fluorophores could be used as singly labeled plasmon-coupled fluorescent probes in high-background biological samples.